Spectroscopic Fingerprint of Phase-Incoherent Superconductivity in the Underdoped $Bi_2Sr_2CaCu_2O_{8+\delta}$

Jhinhwan Lee,[1] K. Fujita,[1,2] A. R. Schmidt,[1] Chung Koo Kim,[1] H. Eisaki,[3] S. Uchida,[2] J. C. Davis[1,4]*

A possible explanation for the existence of the cuprate "pseudogap" state is that it is a d-wave superconductor without quantum phase rigidity. Transport and thermodynamic studies provide compelling evidence that supports this proposal, but few spectroscopic explorations of it have been made. One spectroscopic signature of d-wave superconductivity is the particle-hole symmetric "octet" of dispersive Bogoliubov quasiparticle interference modulations. Here we report on this octet's evolution from low temperatures to well into the underdoped pseudogap regime. No pronounced changes occur in the octet phenomenology at the superconductor's critical temperature T_c, and it survives up to at least temperature $T \sim 1.5\ T_c$. In this pseudogap regime, we observe the detailed phenomenology that was theoretically predicted for quasiparticle interference in a phase-incoherent d-wave superconductor. Thus, our results not only provide spectroscopic evidence to confirm and extend the transport and thermodynamics studies, but they also open the way for spectroscopic explorations of phase fluctuation rates, their effects on the Fermi arc, and the fundamental source of the phase fluctuations that suppress superconductivity in underdoped cuprates.

Superconductivity in the hole-doped CuO_2 Mott insulators is unique by virtue of the convergence of three phenomena. First, the superconductivity is quasi–two-dimensional, because it occurs primarily in the CuO_2 planes. Second, presumably because of correlations, the superfluid density is very low and increases from zero approximately linearly with the hole density p. Third, because it is a d-wave system, the superconducting energy gap $\Delta(\vec{k})$ exhibits four k-space nodes where zero-energy excitations exist. This unique combination means that fluctuations of the quantum phase $\varphi(\vec{r},t)$, where $\vec{r}$ is the position vector and t is time, of the superconducting order parameter $\Psi = \Delta e^{i\varphi(\vec{r},t)}$ should have profound effects on cuprate superconductivity at low hole density (1–6). One might then expect to observe a sequence of three different temperature scales. The highest characteristic temperature would occur at the mean-field scale, T_{MF}, where local pairing begins. The next, T_ϕ, is where strong diamagnetic fluctuations would set in. The lowest is the true superconducting critical temperature, T_c, where phase rigidity would appear in the presence of whatever combination of thermal and quantum fluctuations (7–12) actually exists in underdoped cuprates.

A schematic of the hole-doped cuprate phase diagram is shown in fig. S1A; within the gray shaded pseudogap regime, the approximate region where transport and thermodynamic evidence for phase-incoherent superconductivity has been detected (13–18) is shaded light blue. The techniques used include terahertz transport studies (13), the Nernst effect in thermal transport (14, 15), torque-magnetometry measurements of diamagnetism (16), field dependence of the diamagnetism (17), and zero-bias conductance enhancement in tunnel junctions linking pseudogapped to superconducting samples (18). But the regions designated as containing phase-incoherent superconductivity differ markedly between these studies. Moreover, it has been proposed recently that much of the Nernst signature attributed to phase fluctuations may be due to the appearance of stripes (19). Thus, a direct spectroscopic fingerprint of phase-incoherent d-wave superconductivity could help to identify the precise regions dominated by phase fluctuations. Perhaps more importantly, the associated spectroscopic phenomena might be used to quantify phase fluctuation rates and to discriminate between different quantum fluctuation sources (7–12) causing the loss of phase rigidity, and thus suppression of high-temperature superconductivity, in underdoped cuprates.

Spectroscopic imaging scanning tunneling microscopy (SI-STM) provides one approach to search for a spectroscopic fingerprint of phase-incoherent d-wave superconductivity. With this technique, the local density of states $N(\vec{r},E)$

(where E is energy), the two branches of the Bogoliubov excitation spectrum $\vec{k}_B(\pm E)$, and the superconducting energy gap magnitude $\pm|\Delta(\vec{k})|$ for both filled and empty states can be determined in a single experiment (20–23). This is because a characteristic form of quasiparticle interference (QPI) occurs in cuprate superconductors where the Bogoliubov quasiparticle dispersion $E(\vec{k})$ has banana-shaped constant energy contours (20–23), as shown schematically in fig. S1B. In theory, the k-space locations of the Bogoliubov band minima and maxima, $\vec{k}_B(\pm E)$, coincide with the maxima in the joint density-of-states at the eight tips of these "bananas." Elastic scattering between these eight regions $\vec{k}_j(\pm E)$ ($j = 1,2,\ldots,8$) produces real-space interference modulations in $N(\vec{r},E)$ that are characterized by two sets of seven dispersive wave vectors $\vec{q}_i(\pm E)$ ($i = 1,2,\ldots,7$), where $\vec{q}_i(+E) = \vec{q}_i(-E)$ (fig. S1B). This is referred to as the octet model of cuprate QPI (20–23) and, for $T << T_c$, it is a definitive signature of d-wave superconductivity. When these $\vec{q}_i(E)$ are measured from the Fourier transform of modulations in the differential tunneling conductance maps, $g(\vec{r},E) \equiv dI/dV(\vec{r},E)$, where I is the tunnel current and V is the tunnel-junction bias voltage, the Bogoliubov bands $\vec{k}_B(\pm E)$ and the superconductor's energy gap structure $\pm|\Delta(\vec{k})|$ can be determined (20–23). This technique is unique in that the measured gap $\pm|\Delta(\vec{k})|$ is definitely that of the superconductor and, because the technique uses visualization of interference patterns, it automatically identifies k-space regions having coherent quasiparticles.

A possible signature of phase-incoherent d-wave superconductivity in the pseudogap regime could be the continued existence of this QPI octet phenomenology. This is because, if the quantum phase $\varphi(\vec{r},t)$ of $\Psi = \Delta e^{i\varphi(\vec{r},t)}$ is fluctuating in space and time, then the energy gap magnitude $\pm|\Delta(\vec{k})|$ could still remain largely unchanged so that the particle-hole–symmetric octet of high joint–density-of-states regions generating the QPI would continue to exist. Because an ungapped Fermi arc appears above T_c in underdoped cuprates (24), it is only the remaining gapped regions beyond the tips of the arc that would be available to support any such pseudogap QPI. Indeed, detailed theoretical studies of the QPI phenomenology that would be expected if the pseudogap regime is a phase-incoherent d-wave superconductor bear out this simple picture (25–27). Among their predictions is the existence of a particle-hole–symmetric octet of dispersive QPI modulations, but perhaps the octet might emerge from a k-space region that is different from that in the superconducting phase.

However, as revealed by the pioneering SI-STM studies at temperatures above T_c (28), the detection of the complete octet of dispersive QPI modulations in the pseudogap regime presents severe technical challenges. Because the basic observables are the particle-hole–symmetric dispersions $\vec{q}_i(+E) = \vec{q}_i(-E)$ for the seven wave

[1]Laboratory of Atomic and Solid State Physics, Department of Physics, Cornell University, Ithaca, NY 14853, USA. [2]Department of Physics, University of Tokyo, Bunkyo-ku, Tokyo 113-0033, Japan. [3]Institute of Advanced Industrial Science and Technology, Tsukuba, Ibaraki 305-8568, Japan. [4]Condensed Matter Physics and Material Science Department, Brookhaven National Laboratory, Upton, NY 11973, USA.

*To whom correspondence should be addressed. E-mail: jcdavis@cornell.edu

vectors $\vec{q}_i$, the primary objectives are to achieve high precision in simultaneous measurements of all seven $|\vec{q}_i|$ and of E within the pseudogap regime. Because the uncertainty in energy of a tunneling electron grows rapidly with temperature (exceeding 30 meV at 100 K), precision in the measurement of E requires the lowest possible temperatures. We therefore chose to reduce T_c of our $Bi_2Sr_2Ca_{0.8}Dy_{0.2}Cu_2O_{8+\delta}$ sample to 37 ± 3 K by strong underdoping so that the pseudogap regime could be entered at low temperatures (fig. S1A, inset). Second, adequate $|\vec{q}_i|$ precision for $Bi_2Sr_2CaCu_2O_{8+\delta}$ QPI requires fields of view (FOVs) exceeding 45×45 nm^2, and any smaller FOV will unavoidably create the erroneous impression of nondispersive modulations (21). Thus, all studies herein were made on an FOV exceeding 45×45 nm^2 (for example, fig. S2). Even more challenging (as we show below) is that the intensities for some $\vec{q}_i(E)$ modulations in the pseudogap regime diminish by more than a factor of 10 compared with the superconducting state, so that greatly increased signal-to-noise ratios for all $g(\vec{r},E)$ measurements are required. To achieve this increased ratio, we acquired each $g(\vec{r},E)$ map for up to 10 days by using a specially designed low-noise preamplifier, a highly drift- and temperature-stabilized STM system, and a replicating single-atom tip preparation technique. Finally, because the truly nondispersive electronic structure of the high-energy states (23, 29) is projected onto the low-energy $g(\vec{r},E)$ by the systematic junction formation error (22, 23), the resulting spurious appearance of nondispersive signals at low bias is avoided here by the use of the relation $Z(\vec{r},E) \equiv g(\vec{r},+E)/g(\vec{r},-E)$ for all QPI analyses (22). Using $Z(\vec{r},E)$ and $Z(\vec{q},E)$ also has the advantage that it automatically extracts particle-hole symmetric $\vec{q}_i(+E) = \vec{q}_i(-E)$ QPI modulations (22, 23).

By combining all these capabilities in a specially designed, variable-temperature SI-STM system, we were able to study the temperature evolution of the octet of QPI modulations in $Z(\vec{q},E)$ from the superconducting phase into the pseudogap regime. The octet of interference modulations was studied at temperatures $T = 4.5, 15, 30, 37, 45,$ and 55 K, thereby entering well into the strongly underdoped pseudogap regime (fig. S1A). We measured the $g(\vec{r},E)$ images with subatomic resolution (fig. S2) on a single $Bi_2Sr_2Ca_{0.8}Dy_{0.2}Cu_2O_{8+\delta}$ sample with $p = 7 \pm 1\%$. This data set consists of $\sim 5 \times 10^5$ atomically resolved and registered tunneling spectra and is described in the supporting online material (SOM) for every temperature T, in terms of a comprehensive set of $Z(\vec{r},E)$ images (fig. S3) and the related $Z(\vec{q},E)$ movies (movies S1 to S6).

Representative $Z(\vec{q},E)$ for six temperatures are shown in Fig. 1. Several important observations can be made from these data. First, the set of $\vec{q}_i(E)$ ($i = 1,2,\ldots,7$) that is characteristic of the superconducting octet model is preserved unchanged upon passing above T_c and exists up to at least $T \sim 1.5T_c$ [compare, for example, (A) and (U)]. This result demonstrates that the QPI octet phenomenology exists in the pseudogap regime. Second, the existence of such interference patterns indicates that coherent wavelike quantum states occur in some parts of k-space in the pseudogap regime. Third, the octet of QPI wave vectors are quantitatively different at different temperatures, indicating that they are generated by different regions of k-space, and thus that $\Delta(\vec{k})$ is evolving with temperature. Fourth, some, but not all, QPI modulation intensities become far weaker in the pseudogap regime.

The measured values of $|\vec{q}_1(E)|$, $|\vec{q}_5(E)|$, and $|\vec{q}_7(E)|$ at each temperature shown in Fig. 2 reveal that the modulations that are dispersive in the superconducting phase (20–23) remain dispersive into the pseudogap regime. This is equally true for every measured octet wave vector (see fig. S4 and movies S1 to S6). Moreover, if d-wave energy gaps without particle-hole symmetry were generating these pseudogap QPI effects, instead of the 16 pairs of modulation wave vectors observed here, $Z(\vec{q},E)$ should exhibit 32 pairs because then, $\vec{q}_i(+E) \neq \vec{q}_i(-E)$. These obser-
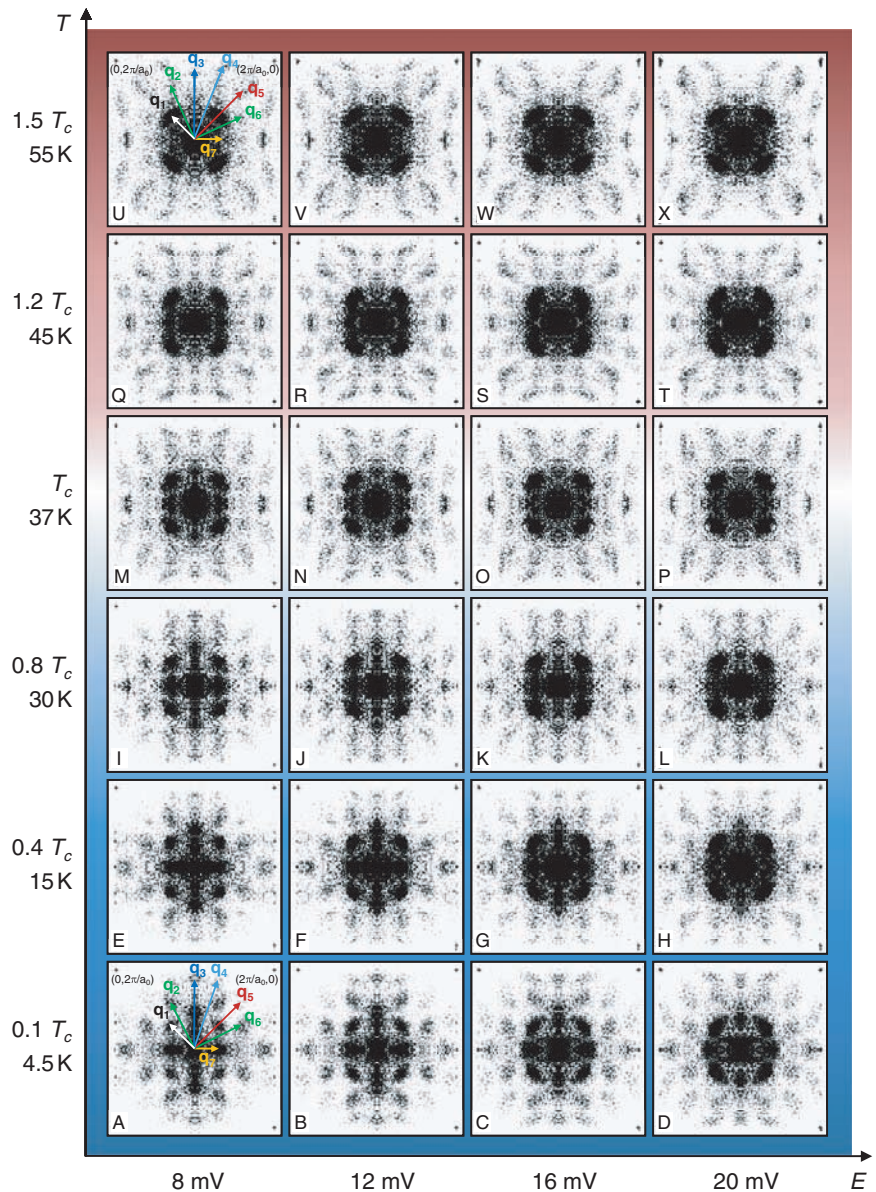

Fig. 1. (**A** to **X**) Differential conductance map $g(\vec{r},E) = dI/dV(\vec{r},E = eV)$ were obtained on the same sample in an atomically resolved and registered FOV > 45×45 nm^2 at six temperatures (fig. S2). Each panel shown is the Fourier transform $Z(\vec{q},E)$ of $Z(\vec{r},E) \equiv g(\vec{r},+E)/g(\vec{r},-E)$ for a given energy and temperature (fig. S3). The QPI signals evolve dispersively with energy along the horizontal energy axis. The temperature dependence of QPI for a given energy evolves along the vertical axis. The octet-model set of QPI wave vectors is observed for every E and T (see movies S1 to S6) as seen, for example, by comparing (A) and (U), each of which has the labeled octet vectors. Within the basic octet QPI phenomenology, there is no particular indication in these data of where the superconducting transport T_c occurs.

vations are important for discrimination between any static electronic ordered state having non-dispersive modulations at an ordering wave vector $\vec{Q}$ and the dispersive k-space eigenstates of a phase-incoherent d-wave superconductor. Because we find that for $|E| < 35$ meV, all detected $\vec{q}_i(E)$ in the pseudogap regime are dispersive and particle-hole symmetric (Fig. 2 and fig. S4) and, moreover, that the dispersions are internally consistent with the octet model (fig. S4), we conclude that these low-energy modulations
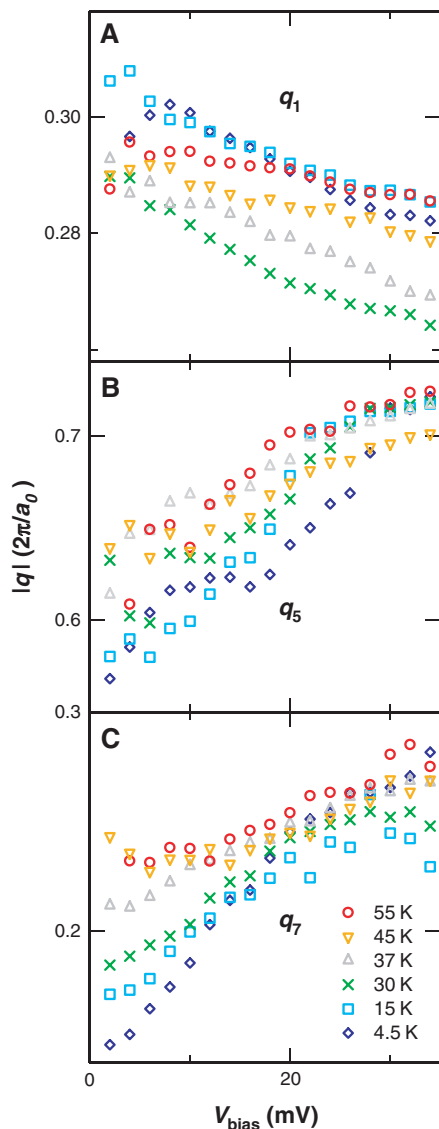
in $Z(\vec{q},E)$ do not represent the signature of any static, electronic ordered state. However, the true nondispersive excitations of underdoped cuprates (23, 29), which occur at the pseudogap energy scale (near $E \sim \pm 120$ meV in this sample) and break translational and rotational symmetry locally, remain completely unaltered upon the transition through T_c into the pseudogap regime (fig. S7).

By requiring octet-model internal consistency (20–23) in the dispersions of all measured $\vec{q}_i(E)$ for all energies and all temperatures (fig. S4), we can determine $\vec{k}_B(\pm E)$ and $|\Delta(\vec{k})|$ as a function of T. The results shown in Fig. 3A (and figs. S5 and S6) indicate that, even at the lowest temperatures, the locus of scattering $\vec{k}_B(E)$ exhibits the ungapped arc previously reported in (22, 23, 30). Beyond the tips of this arc are the gapped regions that exhibit particle-hole–symmetric QPI, which then disappears at the line connecting $(\pi/a_0,0)$ and $(0,\pi/a_0)$ (23). Beyond that line, the electronic excitations to the pseudogap energy scale exhibit locally broken translational and rotational symmetries in r-space (23, 29). Figure 3A shows the

energy gap $|\Delta(\vec{k})|$ measured using the standard octet analysis (20–23) as a function of temperature. We see that, whereas the measured $\vec{k}_B(E)$ are on the same contour in k-space at all T (fig. S5), the ungapped arc length grows slowly with increasing T and the gapped regions exhibiting octet QPI thereby become more constricted in k-space (fig. S6). Figure 3B shows that the ungapped arc length is a monotonically increasing function of temperature (figs. S6 and S8). Moreover, the simultaneously measured zero-bias conductance shown in Fig. 3B (which is proportional to the density of states at the Fermi energy shown in Fig. 3C) also exhibits a high value at lowest temperatures and increases linearly with T. This result provides additional evidence for an ungapped zero-temperature arc that lengthens linearly with T. If such an ungapped arc in the superconducting state can be generated either by scattering (31, 32) or by non-thermally generated phase fluctuations (6), then these results appear to be consistent with the linear increase in Fermi arc length with temperature that
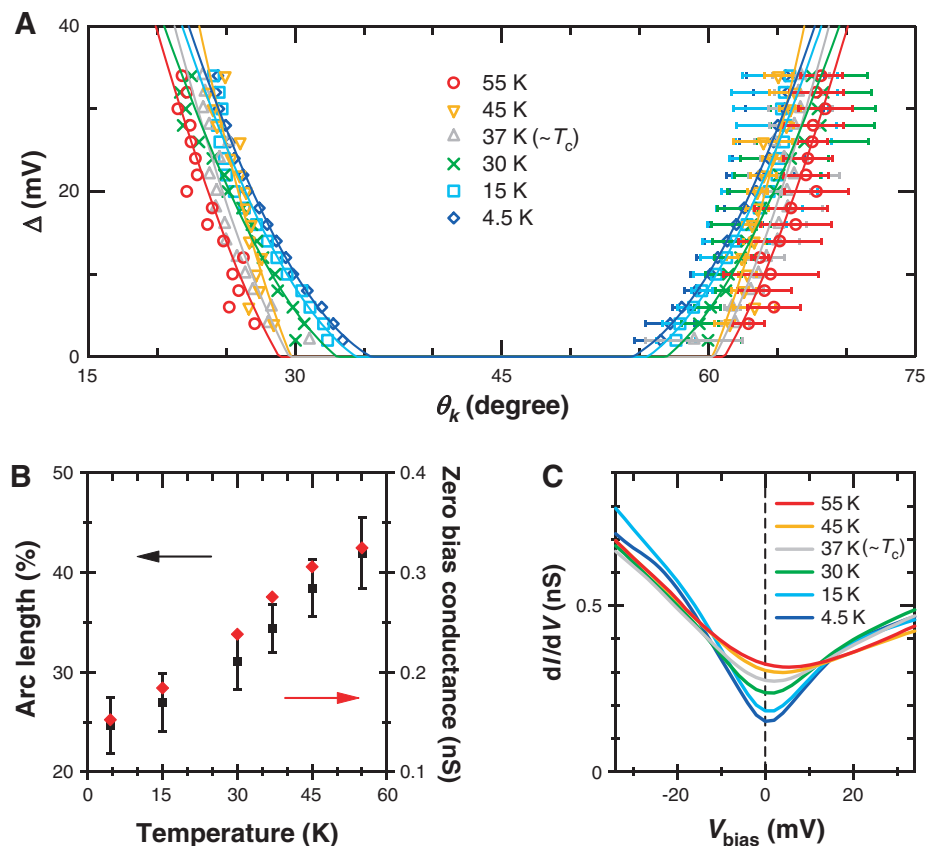

Fig. 2. (**A** to **C**) Temperature dependence of the length of representative q-vectors—$|\vec{q}_1(E)|$, $|\vec{q}_5(E)|$, and $|\vec{q}_7(E)|$—as a function of energy. We show here and in fig. S4 and movies S1 to S6 that octet modulation vectors $\vec{q}_1$, $\vec{q}_2$, $\vec{q}_4$, $\vec{q}_5$, $\vec{q}_6$, and $\vec{q}_7$ are manifestly dispersive at all temperatures studied, with the gradual changes in length as temperature is increased (fig. S3). Wave vector $\vec{q}_3$ has been difficult to observe at all energies and so is not used in the QPI analysis. Wave vector $\vec{q}_5$ is easily detected and is dispersive as expected; however, it contains a second-order contribution and so is not used in the determination of $\pm|\Delta(\vec{k})|$.

Fig. 3. (**A**) The superconducting energy gap $\pm|\Delta(\vec{k})|$ to coherent k-space Bogoliubov quasiparticle excitations [as determined from the internally consistent octet model analysis of $Z(\vec{q},E)$] in the superconducting phase is shown for temperatures 4.5, 15, and 30 K. The energy gap magnitude $\pm|\Delta(\vec{k})|$ to coherent k-space excitations in the nonsuperconducting phase or pseudogap regime is shown for temperatures 37, 45, and 55 K. (**B**) The ungapped arc length from QPI analysis shows approximately linear temperature dependence. As previously reported in (22, 23, 30), there is an ungapped region even at the lowest temperatures in the superconducting state and, based on the observations shown here, this is probably indicative of combined effects of disorder and phase fluctuations from quantum mechanical sources. (**C**) The spatially averaged differential conductance is plotted as a function of temperature measured simultaneously with the data shown in Fig. 1. The high value of the zero-bias conductance is apparent even at low temperatures.

was originally observed in the pseudogap regime at higher doping (33).

We have emphasized that little distinguishes the observed octet QPI phenomenology between the superconducting phase and the underdoped pseudogap region (Figs. 1 to 3). However, Fig. 4 shows analysis of the energy and temperature dependence of the amplitudes of modulations due to scattering between k-space regions that have the same sign of the d-wave order parameter and between regions of opposite sign. Whereas the latter intensities drop precipitously as T rises (Fig. 4, B to D), the former pass right through T_c without appreciable changes (Fig. 4, F to H). This could be consistent with the d-wave Bogoliubov quasiparticle scattering processes, whose coherence factor products are insensitive to order parameter sign changes (30), remaining unperturbed by the loss of long-range phase rigidity in the pseudogap regime.

With the high $|\vec{q}|$ and E resolution and the enhanced sensitivity to very weak conductance variations introduced here, we were able to find the following characteristics for the low-energy quasiparticle interference modulations in the underdoped cuprate pseudogap regime: (i) The set of seven $\vec{q}_i(E)$ (i = 1,2,…,7) that are characteristic of the superconducting octet model are preserved unchanged upon passing above T_c (Fig. 1 and fig. S4). (ii) All the $\vec{q}_i(E)$ remain dispersive in a manner that is internally consistent with the octet phenomenology (Fig. 2 and fig. S4). (iii) The octet modulation wave vectors retain their particle-hole symmetry $\vec{q}_i(+E) = \vec{q}_i(-E)$. (iv) The modulations occur in the same energy range and emanate from the same contour in k-space (although at varying locations on that contour) as those observed at lowest temperatures (Fig. 3 and fig. S5). (v) The particle-hole–symmetric energy gap $\pm|\Delta(\vec{k})|$ moves away from the nodes with increasing T, leaving behind a growing arc of gapless excitations (Fig. 3). (vi) The intensities of modulations due to scattering between k-space regions having the same sign of a d-wave order parameter are maintained, whereas the intensities of those having a different sign are greatly diminished (Fig. 4).

These observations represent a number of advances in our understanding of the electronic structure of the cuprate pseudogap regime. First, because the basic QPI octet phenomenology is definitely the signature of d-wave superconductivity well below T_c (20–23), and because we show here that it evolves without pronounced changes through T_c, it seems implausible that it represents a different state above T_c. Moreover, the observed particle-hole–symmetric, dispersive, octet-model phenomenology is consistent with theoretical predictions for the QPI characteristics of a phase-incoherent d-wave superconductor (25–27). Our data therefore provide spectroscopic evidence confirming and extending the deductions reached in the transport and thermodynamic studies (13–17). In addition, knowledge of this spectroscopic signature may

now make it possible to explore the phase diagram regions exhibiting this state, to quantify the phase fluctuation rates with changing temperature (6) and doping, and to discriminate between different quantum fluctuation sources (7–12). Second, because all the $\vec{q}_i(E)$ observed in $Z(\vec{q},E)$ disperse internally consistently with the octet model, they do not represent the signature of a static, ordered state in the underdoped pseudogap regime. Nevertheless, it is equally important to emphasize that the true nondispersive and symmetry-breaking excitations that occur at the
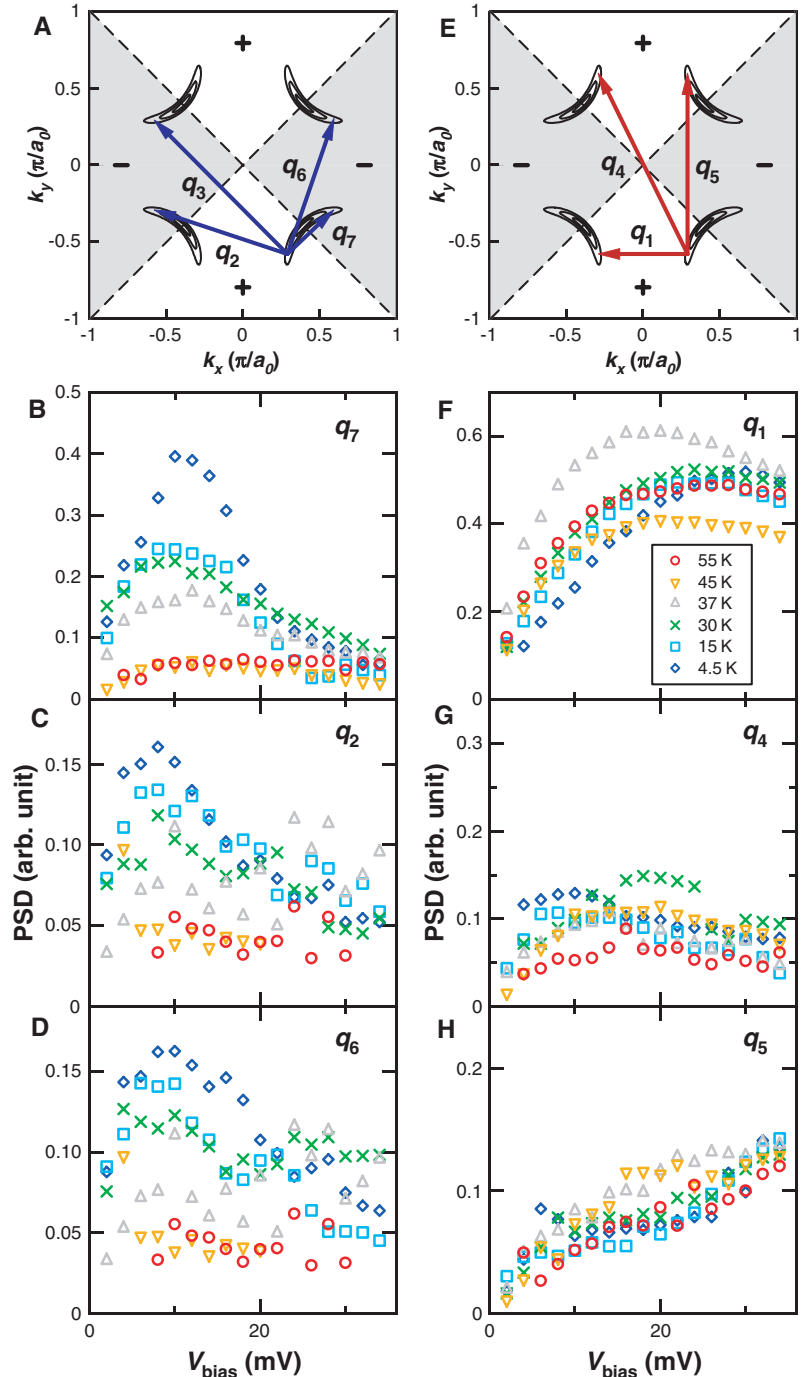

Fig. 4. (**A**) The octet q-vectors due to scattering between regions of k-space with different signs of a d-wave order parameter are indicated. (**B** to **D**) The power spectral densities for modulations with q_7, q_2, and q_6 at each energy and for different temperatures are shown. These modulations show a rapid decrease in intensity as temperature is increased. (**E**) The octet q-vectors due to scattering between regions of k-space with the same sign of a d-wave order parameter are indicated. (**F** to **H**) The power spectral densities for modulations q_1, q_4, and q_5 at each energy and for different temperatures are plotted. The intensity of these modulations shows no trend as temperature is increased and no particular indication of where the transport T_c occurs.

pseudogap energy scale (*23*, *29*) coexist with these low-energy dispersive modulations at all temperatures studied. Third, analysis of the data using the octet model provides a new perspective on the superconducting energy gap at lowest dopings, indicating that an arc of gapless excitations exists in the strongly underdoped superconducting phase (*22*, *23*, *30*) and that it expands linearly in temperature. Such an arc might exist either due to effects of scattering (*31*, *32*) or due to phase fluctuations (*6*) that are generated by a purely quantum mechanical processes (*7–12*, *34*), or both. Fourth, as the alterations in interference intensities (Fig. 4) that are detected with increasing temperature mimic those generated by introduction of static vortices at low temperatures (*30*), it may be that they occur here for similar reasons but now in a nonstatic vortex fluid (*13–17*). Finally, our observations reveal that the electronic structure of the strongly underdoped pseudogap regime contains not two, but three fundamental components: (i) the Fermi arc (*24*), (ii) the gap $\pm|\Delta(\vec{k})|$ of a phase-disordered superconductor to coherent *k*-space excitations, and (iii) the nondispersive and locally symmetry-breaking excitations at the pseudogap energy scale (*23*, *29*).

References and Notes
1. M. Randeria, N. Trivedi, A. Moreo, R. T. Scalettar, *Phys. Rev. Lett.* **69**, 2001 (1992).
2. V. J. Emery, S. A. Kivelson, *Nature* **374**, 434 (1995).
3. M. Franz, A. J. Millis, *Phys. Rev. B* **58**, 14572 (1998).
4. E. W. Carlson, S. A. Kivelson, V. J. Emery, E. Manousakis, *Phys. Rev. Lett.* **83**, 612 (1999).
5. H.-J. Kwon, A. T. Dorsey, P. J. Hirschfeld, *Phys. Rev. Lett.* **86**, 3875 (2001).
6. E. Berg, E. Altman, *Phys. Rev. Lett.* **99**, 247001 (2007).
7. M. Franz, Z. Tešanović, *Phys. Rev. Lett.* **87**, 257003 (2001).
8. I. F. Herbut, *Phys. Rev. Lett.* **88**, 047006 (2002).
9. M. Hermele, T. Senthil, M. P. A. Fisher, *Phys. Rev. B* **72**, 104404 (2005).
10. E.-A. Kim et al., *Phys. Rev. B* **77**, 184514 (2008).
11. A. Pelissetto, S. Sachdev, E. Vicari, *Phys. Rev. Lett.* **101**, 027005 (2008).
12. M. Grilli, G. Seibold, A. D. Ciolo, J. Lorenzana, *Phys. Rev. B* **79**, 125111 (2009).
13. J. Corson, R. Mallozzi, J. Orenstein, J. N. Eckstein, I. Bozovic, *Nature* **398**, 221 (1999).
14. Z. A. Xu, N. P. Ong, Y. Wang, T. Kakeshita, S. Uchida, *Nature* **406**, 486 (2000).
15. Y. Wang, L. Li, N. P. Ong, *Phys. Rev. B* **73**, 024510 (2006).
16. Y. Wang et al., *Phys. Rev. Lett.* **95**, 247002 (2005).
17. L. Li et al., *Europhys. Lett.* **72**, 451 (2005).
18. N. Bergeal et al., *Nat. Phys.* **4**, 608 (2008).
19. O. Cyr-Choinière et al., *Nature* **458**, 743 (2009).
20. J. E. Hoffman et al., *Science* **297**, 1148 (2002).
21. K. McElroy et al., *Nature* **422**, 592 (2003).
22. T. Hanaguri et al., *Nat. Phys.* **3**, 865 (2007).
23. Y. Kohsaka et al., *Nature* **454**, 1072 (2008).
24. M. R. Norman et al., *Nature* **392**, 157 (1998).
25. T. Pereg-Barnea, M. Franz, *Phys. Rev. B* **68**, 180506 (2003).
26. S. Misra, M. Vershinin, P. Phillips, A. Yazdani, *Phys. Rev. B* **70**, 220503 (2004).
27. D. Wulin, Y. He, C.-C. Chien, D. K. Morr, K. Levin, *Condens. Matt.*, preprint available at http://arxiv.org/abs/0904.3114v1 (2009).
28. M. Vershinin et al., *Science* **303**, 1995 (2004).
29. Y. Kohsaka et al., *Science* **315**, 1380 (2007).
30. T. Hanaguri et al., *Science* **323**, 923 (2009).
31. S. Haas, A. V. Balatsky, M. Sigrist, T. M. Rice, *Phys. Rev. B* **56**, 5108 (1997).
32. A. V. Chubukov, M. R. Norman, A. J. Millis, E. Abrahams, *Phys. Rev. B* **76**, 180501(R) (2007).
33. A. Kanigel et al., *Nat. Phys.* **2**, 447 (2006).
34. I. Hetel, T. R. Lemberger, M. Randeria, *Nat. Phys.* **3**, 700 (2007).
35. We acknowledge and thank J. C. Campuzano, T. Hanaguri, M. Franz, P. J. Hirschfeld, D.-H. Lee, S. Kivelson, Y. Kohsaka, E.–A. Kim, M. Lawler, J. Lee, K. Levin, D. Morr, M. Norman, N. P. Ong, J. Orenstein, M. Randeria, S. Sachdev, H. Takagi, and A. Tsvelik for helpful discussions and communications. These studies are supported by Brookhaven National Laboratory, the U.S. Department of Energy, the U.S. Office of Naval Research, by Grant-in-Aid for Scientific Research from the Ministry of Science and Education (Japan), and by the Global Centers of Excellence Program for Japan Society for the Promotion of Science. A.S. acknowledges support from the U.S. Army Research Office.

Strong Coupling Between Single-Electron Tunneling and Nanomechanical Motion

G. A. Steele,* A. K. Hüttel,† B. Witkamp, M. Poot, H. B. Meerwaldt, L. P. Kouwenhoven, H. S. J. van der Zant

Nanoscale resonators that oscillate at high frequencies are useful in many measurement applications. We studied a high-quality mechanical resonator made from a suspended carbon nanotube driven into motion by applying a periodic radio frequency potential using a nearby antenna. Single-electron charge fluctuations created periodic modulations of the mechanical resonance frequency. A quality factor exceeding 10^5 allows the detection of a shift in resonance frequency caused by the addition of a single-electron charge on the nanotube. Additional evidence for the strong coupling of mechanical motion and electron tunneling is provided by an energy transfer to the electrons causing mechanical damping and unusual nonlinear behavior. We also discovered that a direct current through the nanotube spontaneously drives the mechanical resonator, exerting a force that is coherent with the high-frequency resonant mechanical motion.

Nanomechanical systems (*1*, *2*) have promising applications, such as ultrasensitive mass detection (*3–5*). The combination of a high resonance frequency and a small mass also makes nanomechanical resonators attractive for a fundamental study of mechanical motion in the quantum limit (*6–9*). For a successful observation of quantum motion of a macroscopic object, a high-frequency nanoscale resonator must have low dissipation (which implies a high quality factor *Q*) and a sensitive detector with minimum back-action (i.e., quantum limited) (*10*, *11*). In our experiment, we demonstrate a dramatic back-action that strongly couples a quantum-dot detector to the resonator dynamics of a carbon nanotube, and which, in the limit of strong feedback, spontaneously excites large-amplitude resonant mechanical motion.

Nanomechanical resonators have been created by etching down larger structures. In small devices, however, surfaces effects impose an upper limit on *Q* (*2*). Alternatively, suspended carbon nanotubes can be used to avoid surface damage from the (etching) fabrication process. We recently developed a mechanical resonator based on an ultraclean carbon nanotube with high resonance frequencies of several hundred megahertz and a *Q* exceeding 10^5 (*12*). Here, we use this resonator to explore a strong coupling regime between single-electron tunneling and nanomechanical motion. We followed the pioneering approaches in which aluminum single-electron transistors were used as position detectors (*6–8*) and atomic force microscopy cantilevers as resonators (*13–15*); however, our experiment is in the limit of much stronger electro-mechanical coupling, achieved by embedding a quantum-dot detector in the nanomechanical resonator itself.

Our device consists of a nanotube suspended across a trench that makes electrical contact to two metal electrodes (Fig. 1). Electrons are confined in the nanotube by Schottky barriers at the Pt metal contacts, forming a quantum dot in the suspended segment. The nanotube growth is the last step in the fabrication process, yielding ultraclean devices (*16*), as demonstrated by the fourfold shell filling of the Coulomb peaks (Fig. 1C). We performed all measurements at 20 mK with an electron temperature of ~80 mK.

Kavli Institute of NanoScience, Delft University of Technology, Post Office Box 5046, 2600 GA, Delft, Netherlands.

*To whom correspondence should be addressed. E-mail: g.a.steele@tudelft.nl
†Present address: Institute for Experimental and Applied Physics, University of Regensburg, 93040 Regensburg, Germany.